Astrophysical light scattering problems (PAP316)

Lecture 4b

Karri Muinonen
Academy Professor
Department of Physics, University of Helsinki, Finland

Contents

- Introduction
  - Spherical particles measured
  - Olivine particles measured
- Phenomenological scatterer
  - Scattering phase matrix
- Multiple scattering computations
  - Database of solutions
- Example: Jovian moon Europa
  - Polarization phase curve
- Intermediate conclusions
  - Future prospects
  - Depolarizing scatterers

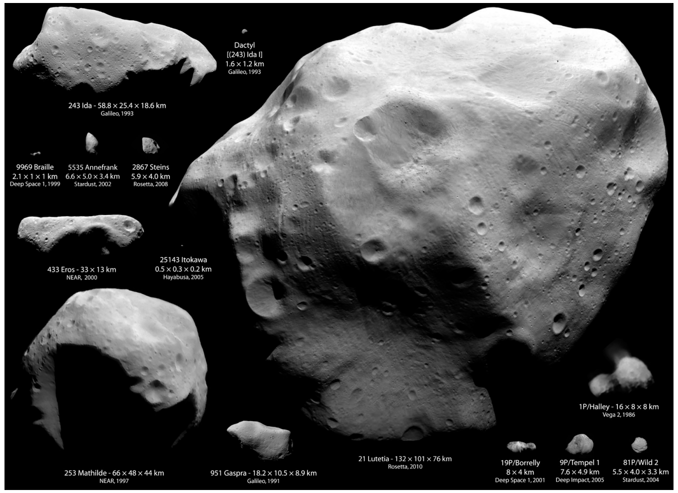

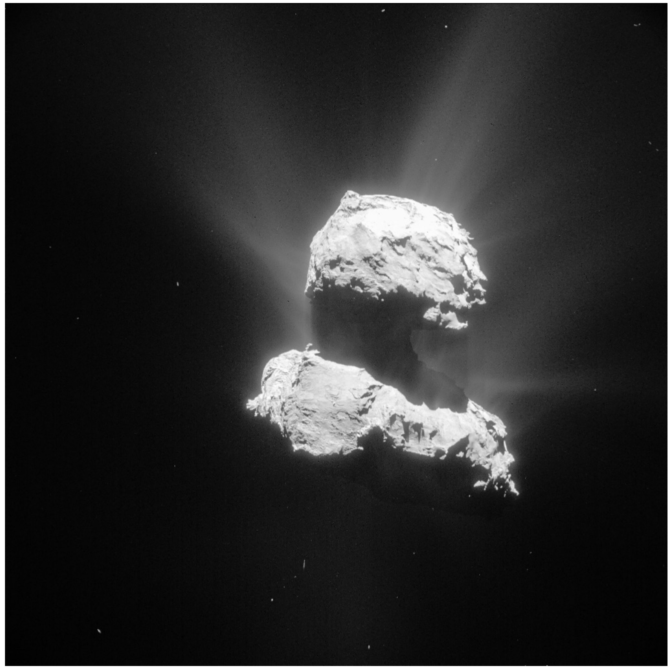

Introduction

- Inverse problem solutions powered by simplified scattering modeling
- Phenomenological scatterer
  - Mathematical model for the scattering phase matrix
  - Retrieval of parameters from observed/measured scattering characteristics
  - Physics-based interpretation of the resulting phase matrix
  - Reference: Muinonen & Videen, JQSRT 113, 2385, 2012

Spherical particles measured

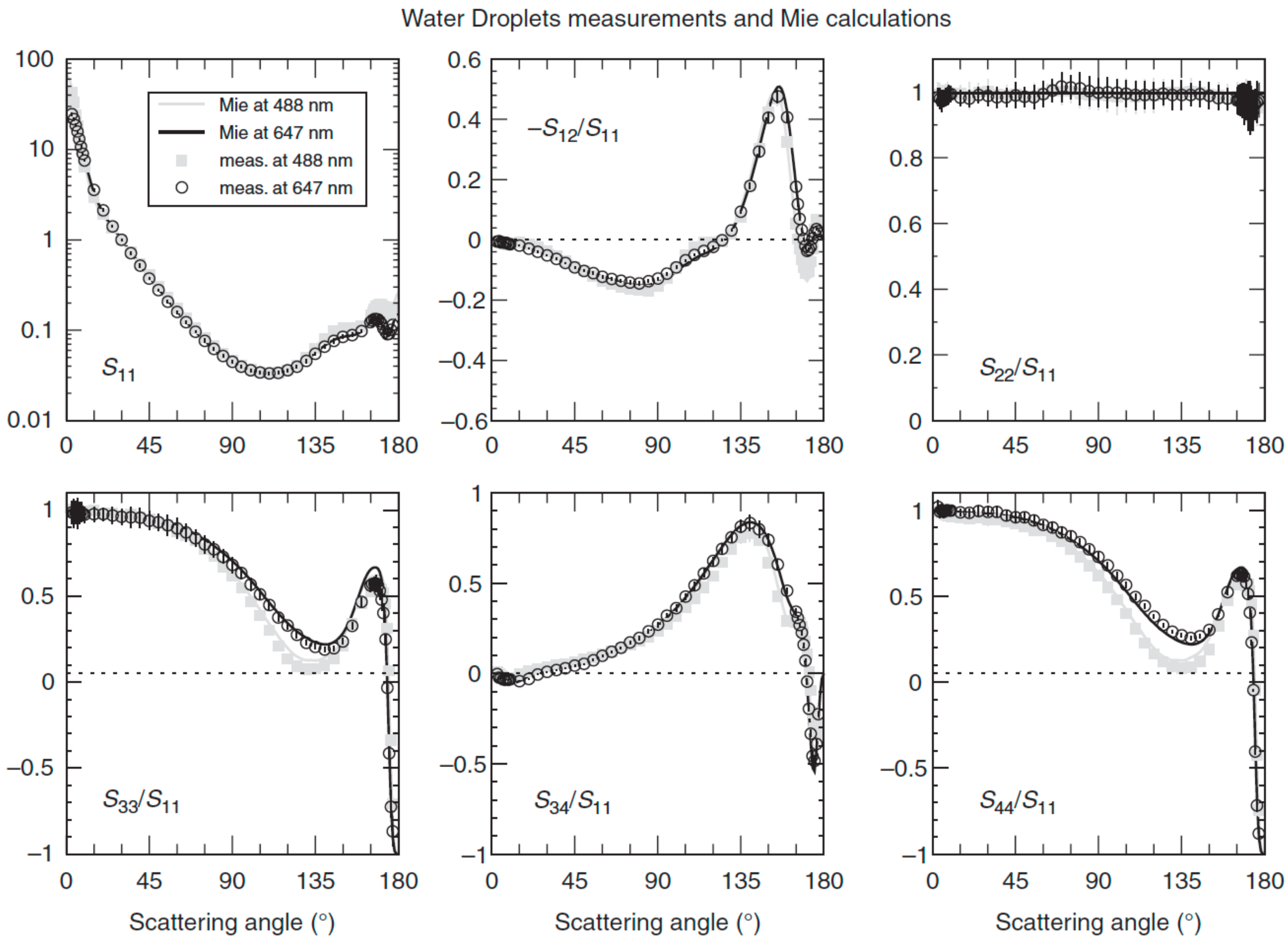

FIGURE 8.3 Comparison of Lorenz–Mie calculations and measured scattering matrix elements for a size distribution of water droplets. The measurements are performed at 488 nm (gray symbols) and 647 nm (black symbols). The S_{11} element is normalized to *1* at 30°.

Olivine particles measured

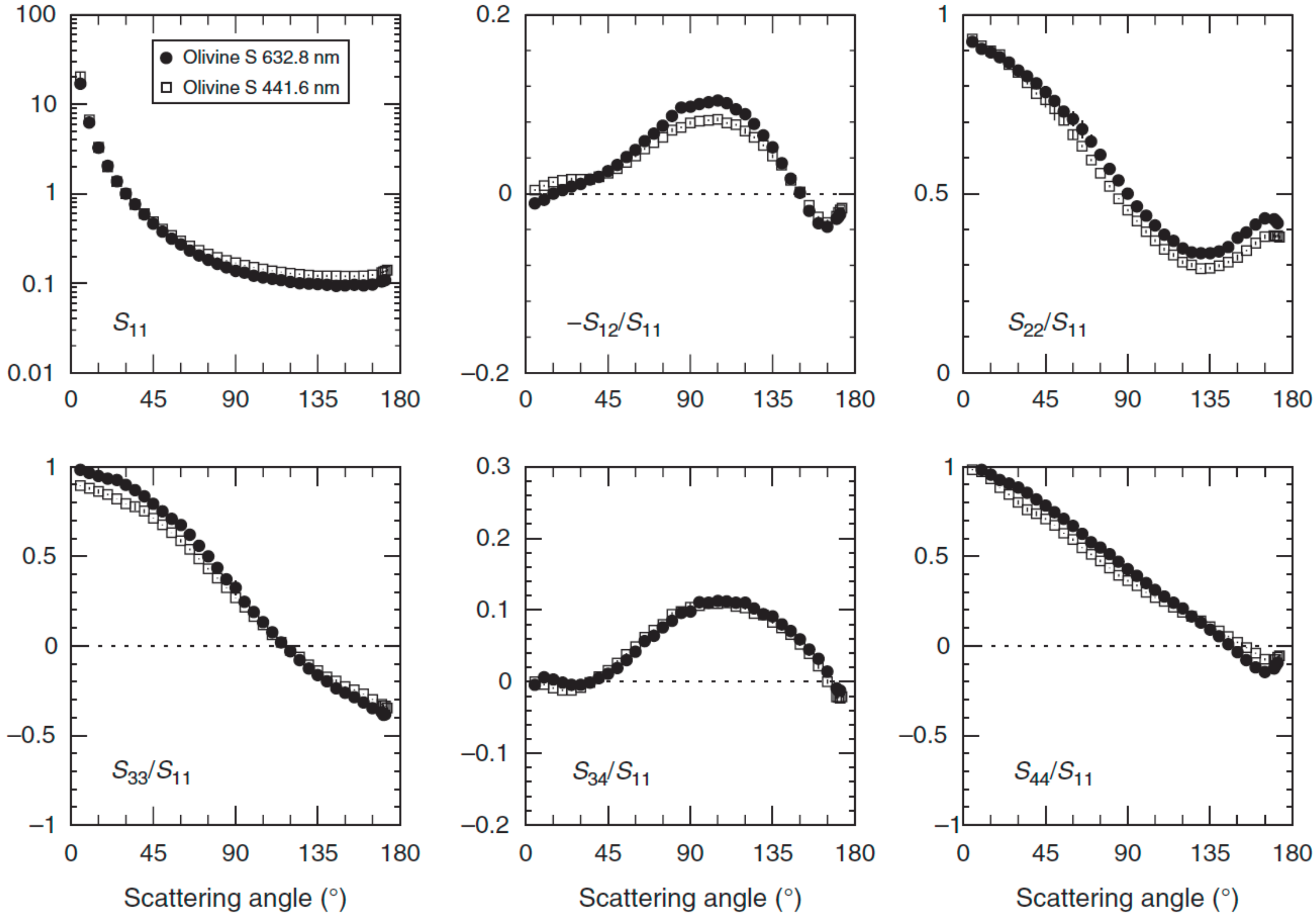

FIGURE 8.7 Measured scattering matrix elements as functions of the scattering angle for a magnesium-rich olivine sample (Olivine S in Muñoz *et al.* 2000). Filled circles and squares correspond to the measurements at 632.8 nm and 441.6 nm, respectively.

Phenomenological scatterer

$$\boldsymbol{P}(\theta) \propto P_{11}(\theta)[w_+\boldsymbol{M}_+(\theta) + w_-\boldsymbol{M}_-(\theta)],\ w_+ + w_- = 1$$

$$\boldsymbol{M}_\pm(\theta) = \begin{pmatrix} 1 & \mp\frac{\sin^2\theta_\pm}{1+\cos^2\theta_\pm} & 0 & 0 \\ \mp\frac{\sin^2\theta_\pm}{1+\cos^2\theta_\pm} & 1 & 0 & 0 \\ 0 & 0 & \frac{2\cos\theta_\pm}{1+\cos^2\theta_\pm} & 0 \\ 0 & 0 & 0 & \frac{2\cos\theta_\pm}{1+\cos^2\theta_\pm} \end{pmatrix}.$$

For $e_+ = e_- = 0$, $\theta_+ = \theta_- = \theta$ and the normalized weight factors

$$w_+ = \tfrac{1}{2}(1 + P_{\max}),$$

$$w_- = \tfrac{1}{2}(1 - P_{\max}), \qquad (4)$$

where $P_{\max}$ gives the maximum for the degree of linear polarization $-P_{12}/P_{11}$ at $\theta = 90^\circ$.

$$P_{11}(\theta) = w\frac{1-g_1^2}{(1+g_1^2-2g_1\cos\theta)^{3/2}} + (1-w)\frac{1-g_2^2}{(1+g_2^2-2g_2\cos\theta)^{3/2}},$$

$$g = wg_1 + (1-w)g_2, \qquad w = \frac{g-g_2}{g_1-g_2},$$

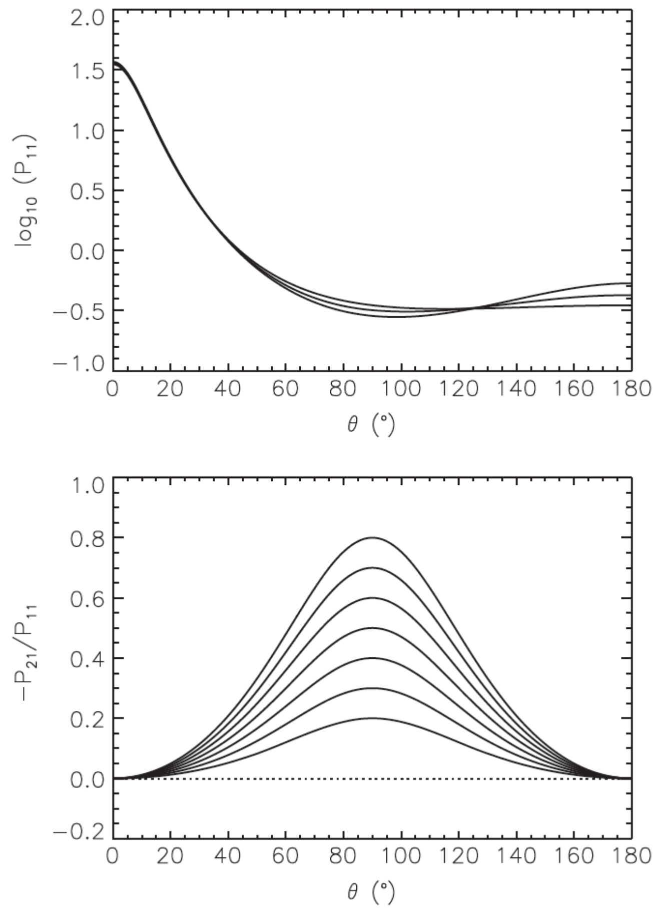

Fig. 1. Double Henyey–Greenstein single-scattering phase function P_{11} (top) and scaled Rayleigh degree of linear polarization for unpolarized incident light $-P_{12}/P_{11}$ (bottom). For the phase functions P_{11}, the total asymmetry parameter is g=0.6 and the forward asymmetry is $g_1 = 0.8$, whereas, in the order of increasing backscattering, the backward asymmetry assumes the values $g_2 = -0.1$, -0.2, and -0.3. For the polarizations $-P_{12}/P_{11}$, the maximum polarization assumes the values $P_{\max} = 0.2, 0.3, \ldots, 0.8$. In addition, $P_{22} = P_{11}$, $P_{33}/P_{11} = P_{44}/P_{11} = \cos\theta$, and $P_{34} = -P_{43} = 0$.

$$\theta_+ - e_+ \sin\theta_+ = \theta,$$

$$\theta_- - e_- \sin\theta_- = \theta.$$

seven parameters: $\tilde{\omega}$, g, g_1, g_2, w_+, e_+, and e_-.

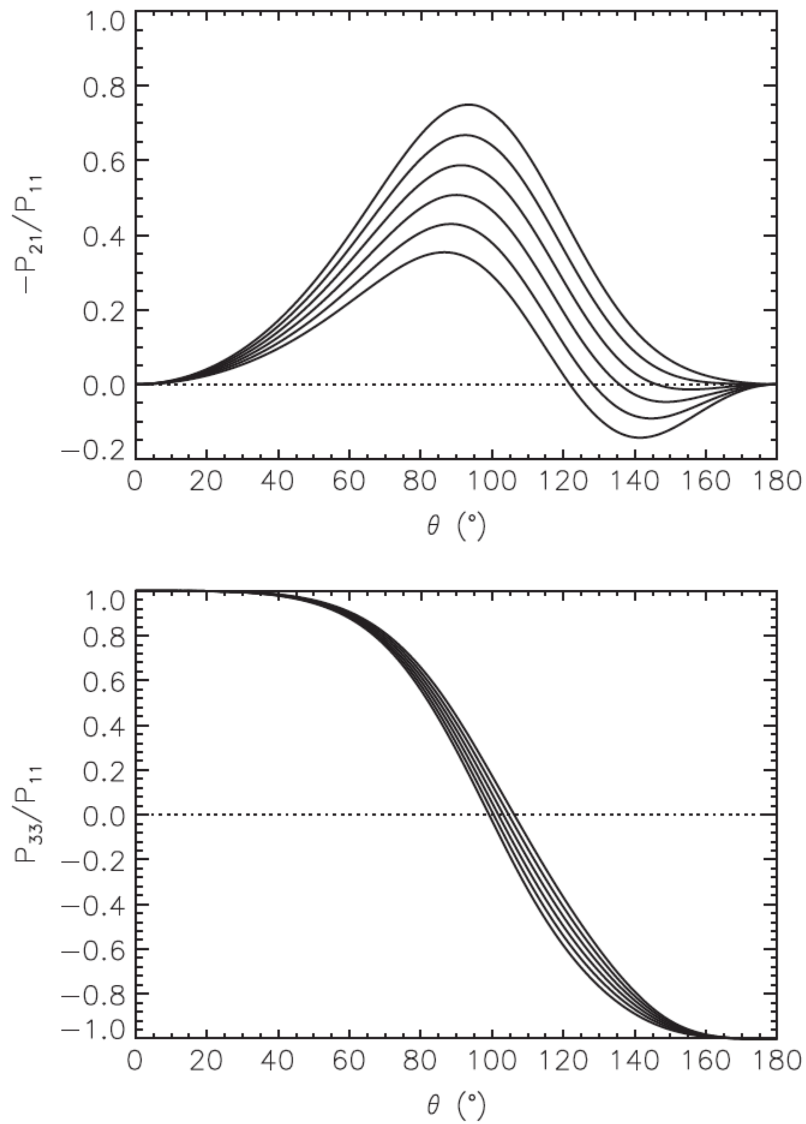

Fig. 2. Degree of linear polarization $-P_{12}/P_{11}$ (top) and P_{33}/P_{11} (bottom) for example negatively polarizing single scatterers. The eccentricities are $e_+ = -0.1$ and $e_- = -0.6$ and the weights are $w_+ = 1 - w_- = 0.60$, 0.65, 0.70, ..., 0.85. With increasing w_+, the polarization $-P_{12}/P_{11}$ increases and P_{33}/P_{11} moves to the left.

Multiple scattering computations

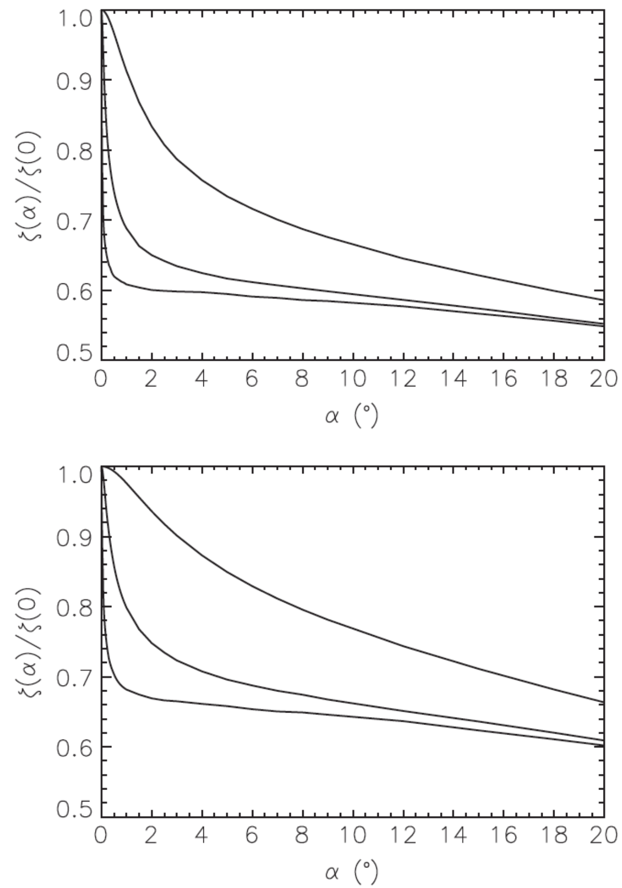

Fig. 3. Coherent-backscattering enhancement factors computed using phenomenological single scatterers with single-scattering albedo $\tilde{\omega} = 0.9$ (top) and 0.6 (bottom) for $k\ell = 30$, 300, and 3000 (large, intermediate, and small angular widths, respectively). In these examples, polarization in single scattering (here $P_{\max} = 0.6$) has a minor effect on the enhancement factors.

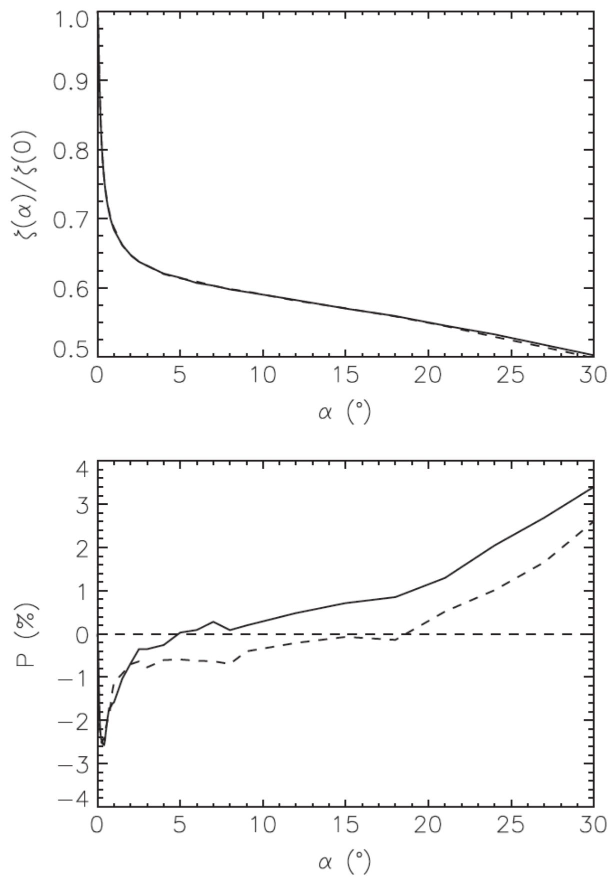

Fig. 5. Enhancement factors (top) and degrees of linear polarization (bottom) computed using phenomenological single scatterers with $\tilde{\omega} = 0.9$ and $w_+ = 1 - w_- = 0.8$. The eccentricities are $e_+ = -0.1$ and $e_- = -0.6$ (solid line; neutral single-scatterer polarization near backscattering) as well as $e_+ = -0.1$ and $e_- = -0.8$ (dashed line; negative single-scatterer polarization near backscattering). The mean free path is $k\ell = 300$.

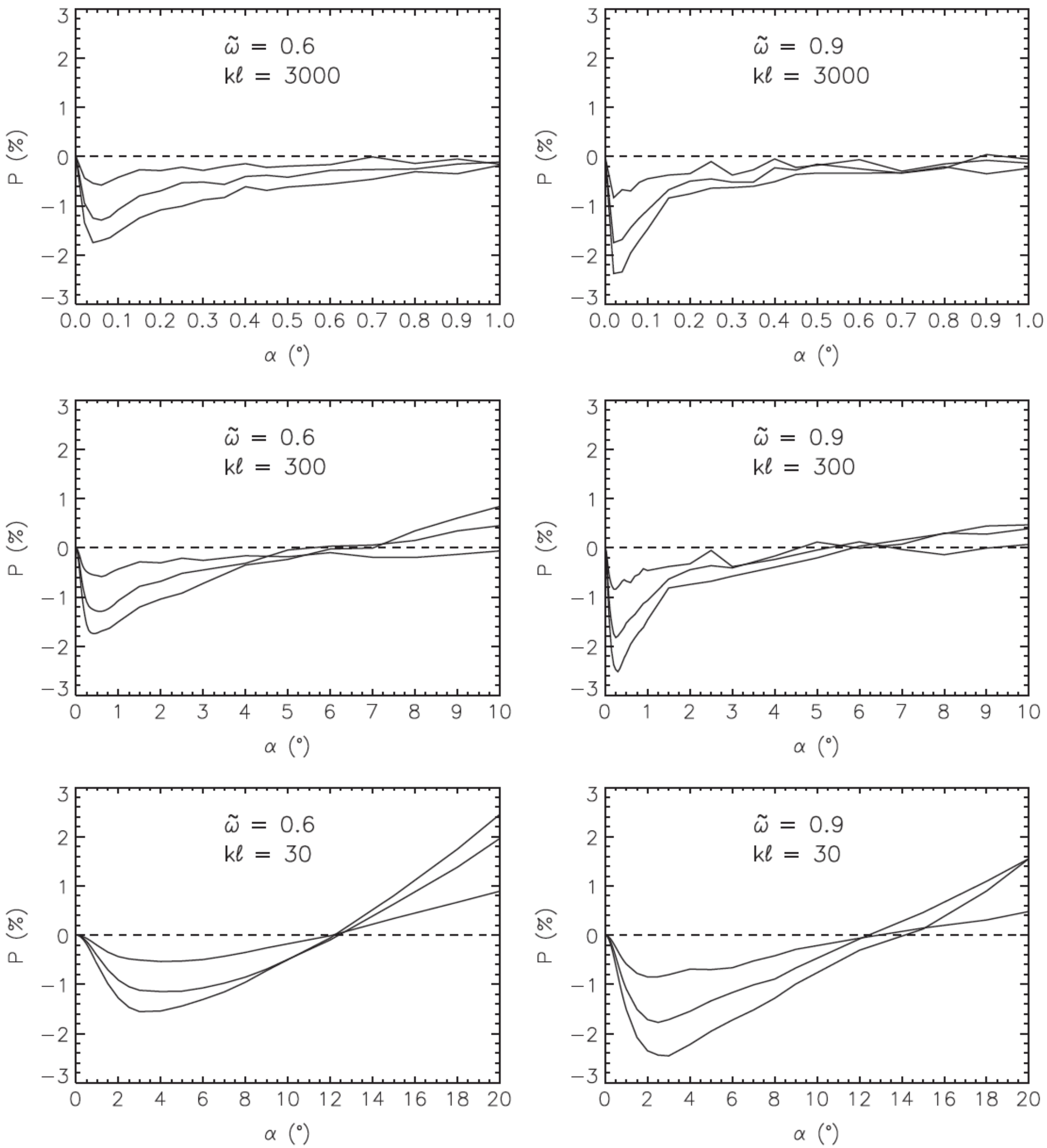

Fig. 4. Degrees of linear polarization for unpolarized incident radiation for $\tilde{\omega} = 0.6$ (left) and 0.9 (right) in the case of $k\ell = 30$ (bottom), 300 (middle), and 3000 (top). The eccentricities $e_+ = e_- = 0$ and the maximum polarization assumes the values $P_{\max} = 0.2$, 0.4, and 0.6 (shallow, intermediate, and pronounced patterns, respectively).

Example: Jovian moon Europa

Kiselev et al., unpublished

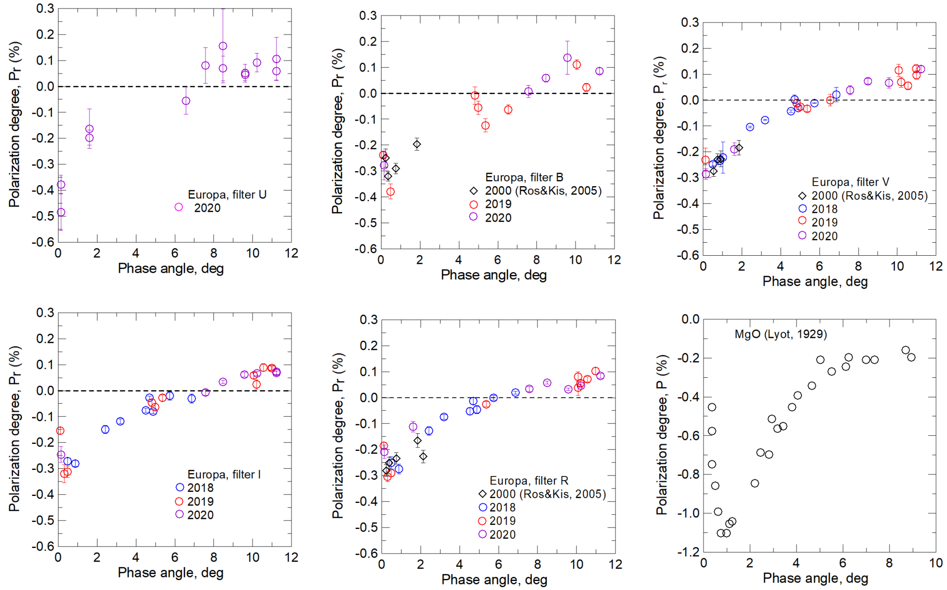

Fig. 2. Phase-angle polarization dependences for Jupiter's satellite Europa in the *UBVRI* filters, obtained in 2018–2020 (open circles) and in 2000 (Rosenbush and Kiselev, 2005) (diamonds). For comparison (bottom row, right panel), the results of laboratory measurements of the polarization of MgO are presented (adopted from the paper by Lyot, 1929).

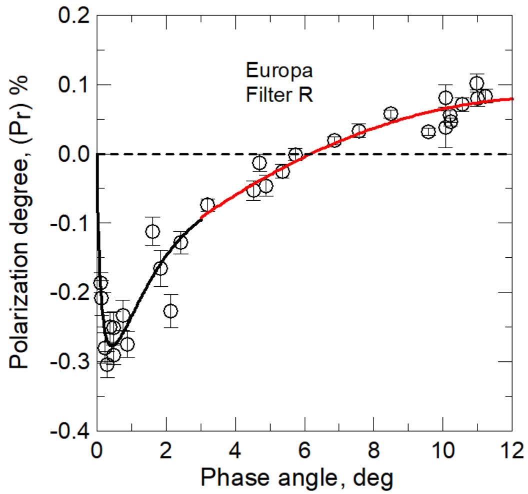

Fig. 3. The fits of Europa's data in the *R* filter taken from Table 4 and Rosenbuch&Kiselev 2005). The black curve is an approximation of data in the phase angle interval ≈(0° – 3°) with expression (7), while the red curve is the fitting of data in the phase angle interval ≈(3° – 12°) with a second-degree polynomial.

kl = 100

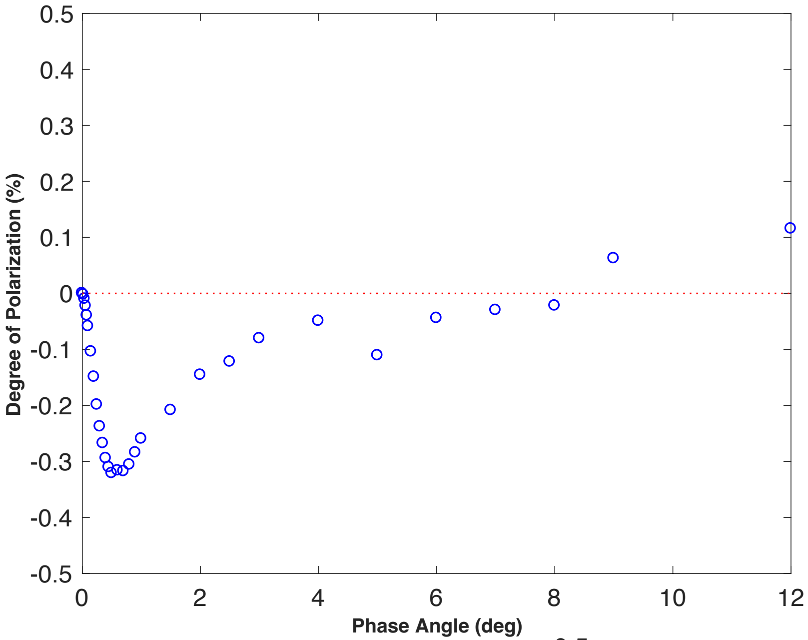

kl = 150

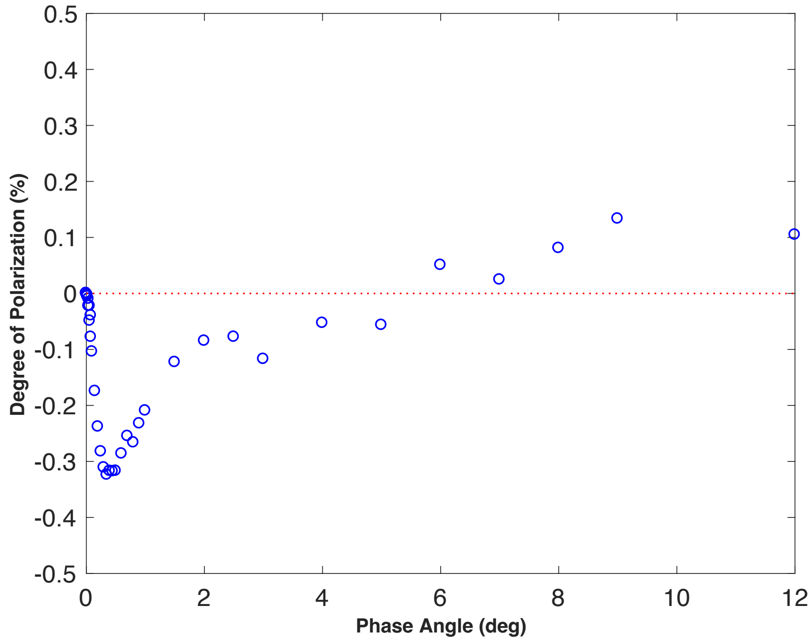

kl = 200

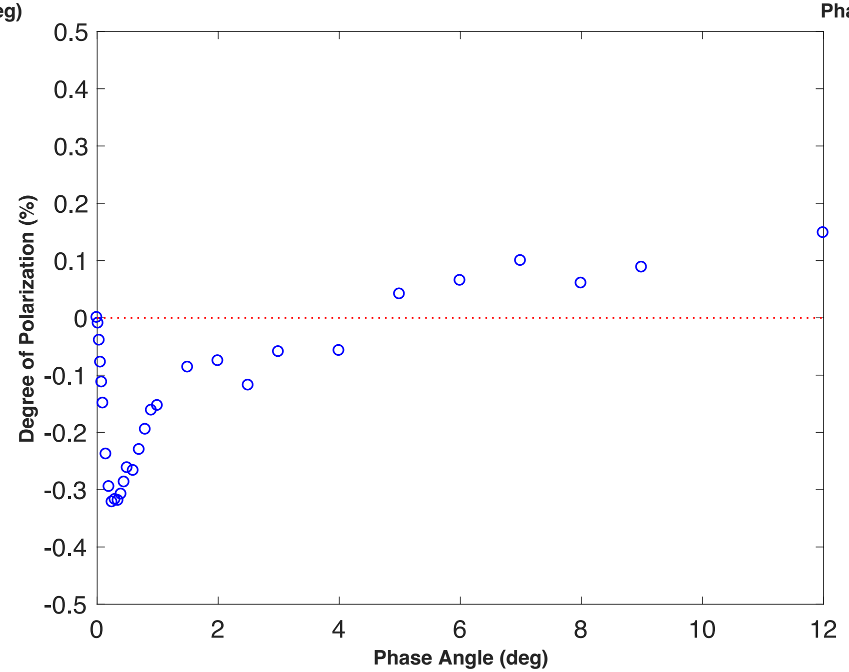

ω = 0.984

P_{max} = 0.08

g = 0.6

g_1 = 0.8

g_2 = -0.1

(p = 0.67-0.68)

Intermediate conclusions

- Extension to measured scattering phase matrices
- Application at large